

Hydrodynamic nuclear analogs with active wave-particle clusters

Rahil N. Valani^{1*} and David M. Paganin²

¹*Rudolf Peierls Centre for Theoretical Physics, Parks Road,
University of Oxford, OX1 3PU, United Kingdom and*

²*School of Physics and Astronomy, Monash University, Victoria 3800, Australia*

(Dated: April 1, 2025)

Active particles are non-equilibrium entities that uptake energy and convert it into self-propulsion. A dynamically rich class of active particles having features of wave-particle coupling and memory are walking/superwalking droplets. Such classical, active wave-particle entities (WPEs) have been shown to exhibit hydrodynamic analogs of many single-particle quantum systems. We numerically investigate the dynamics of several WPEs and find that they self-organize into a bound cluster, akin to a nucleus. This active cluster exhibits various modes of collective excitations as the memory of the system is increased. Dynamically distinct excitation modes create a common time-averaged collective potential indicating an analogy with the bag model of a nucleus. At high memory, the active cluster can destabilize and eject WPEs whose decay statistics follow exponential laws analogous to radioactive nuclear decay. Hydrodynamic nuclear analogs open up new directions to pursue, both experimentally and numerically, within the nascent field of hydrodynamic quantum analogs.

Introduction—The evolution of systems exhibiting memory effects is often governed by integrodifferential equations, which abound in the physics of coupled particle–field systems. For example, in electrodynamics, the Lorentz force acting on each member of a point-charge system leads to an integrodifferential equation for the motion of each particle [1]. As another example, the Dirac equation assumes an integrodifferential form when a single-electron Dirac field is coupled to an electromagnetic field created by the past history of the system [2]. For a classical particle coupled to the field it radiates, the particle interacts locally (i.e., via a finite-order differential equation) with the field created by its past history (as described by an integral superposing Green functions associated with the past states of the system). Of course, when the effects of radiation reaction are weak, one can work with finite-order differential equations by introducing the simplifying approximation that the particle is the “source” which radiates an associated field described via electromagnetic potentials [3–5]. However, when backreaction is strong—i.e., when the particle and its associated field exhibit significant mutual influence upon one another—it is often natural to retain the full complexity of the governing integrodifferential equation. Alternatively, reduced integrodifferential equations may be employed, with examples including the Hartree–Fock equation of elementary quantum mechanics [6] and the “IDEA” formalism in nuclear physics [7–12].

A particular class of matter, known as active matter, has gained considerable physics interest in recent years [14]. Here the individual units are non-equilibrium active particles that consume energy and convert it into persistent motion. Examples includes animate matter from motile micro-scale bacteria to animals and birds, as well as inanimate matter such as active colloids and microrobots [15, 16]. An inanimate hydrodynamic active

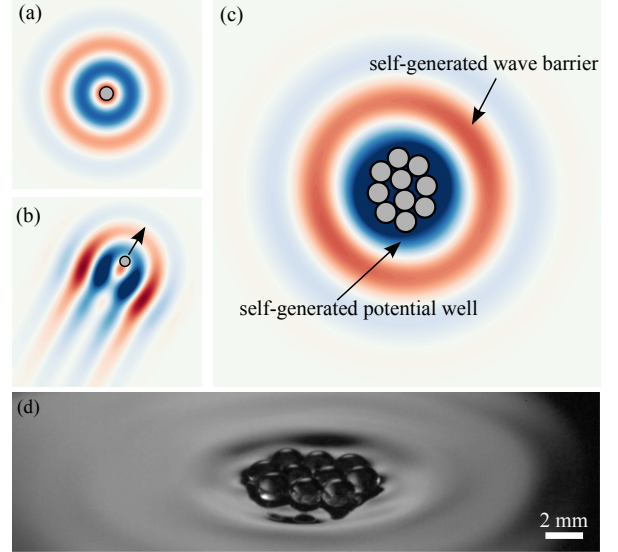


FIG. 1. Active wave-particle cluster. A finite-size particle (gray) generates (a) an axisymmetric wave of form $W(|\mathbf{x}|) = \cos(|\mathbf{x}|) \exp[-(|\mathbf{x}|/2l)^2]$ (peaks in red and troughs in blue) at each instant of time. (b) The superposition of all the individual waves generated by the particle results in an overall wave field that propels an isolated particle with constant velocity (black arrow), making it active. (c) Simulated snapshot in time of a collection of such active WPEs that self-organize into a “nucleus” structure, where the particles stay bound by their self-generated collective wave field comprising a potential well walled by a wave barrier. (d) Experimental image of a self-organized cluster of superwalking droplets [13].

system that exhibits memory effects and can also be described by integrodifferential equations is that of walking/superwalking droplets [13, 17, 18]. In this system, a droplet of oil self-propels horizontally while periodically bouncing on a vertically vibrated bath of the same oil. Each bounce of the droplet excites localized damped standing waves which the droplet interacts with on sub-

* rahil.valani@physics.ox.ac.uk

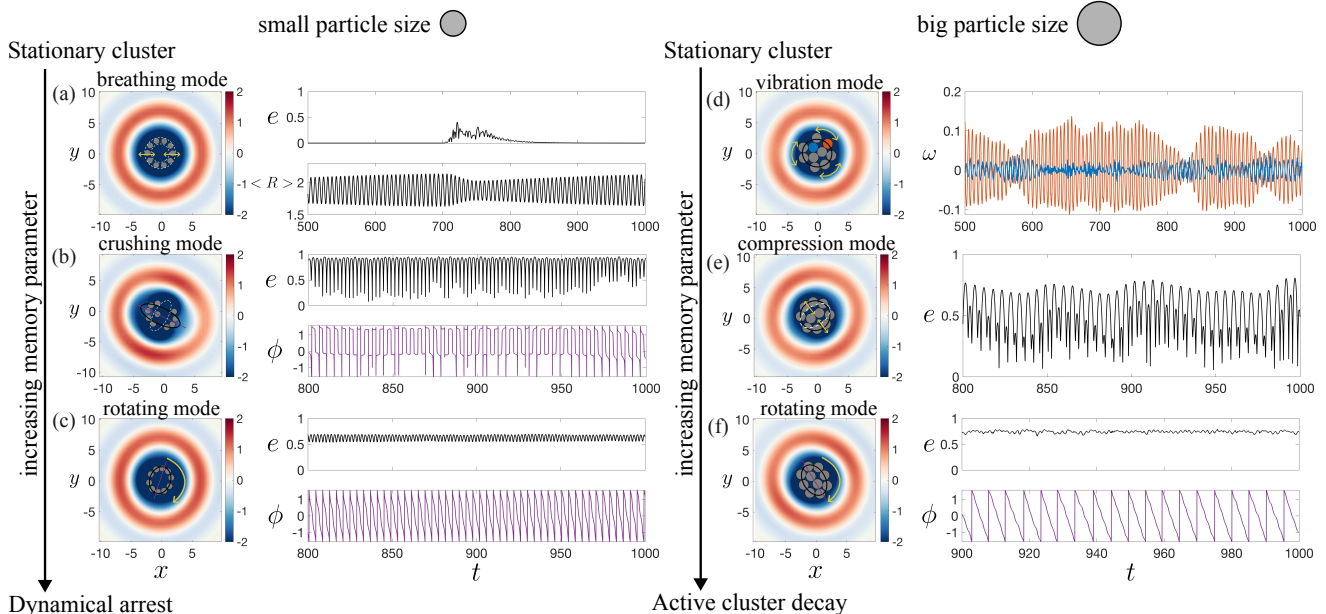


FIG. 2. Collective excitation modes with increasing memory. A cluster of 10 WPEs each with dimensionless diameter $a = 1.01$ is stationary at very small values of the memory parameter τ . With increasing τ and fixed $R = 0.77$, the cluster undergoes different excitation modes such as (a) breathing mode ($\tau = 0.55$), (b) crushing mode ($\tau = 3.27$), (c) rotating mode ($\tau = 7.85$). A cluster of bigger particles with $a = 1.63$ is also stationary for very low τ and undergoes collective excitation with increasing τ for fixed $R = 1.72$, such as (d) vibration mode ($\tau = 0.69$), (e) compression mode ($\tau = 0.83$) and (f) rotating mode ($\tau = 5.24$). Other parameters are fixed to $\alpha = 0.16$. See also Supplemental Videos S1-S6 for videos of modes in (a)-(f).

sequent bounces to propel itself. This active system is dynamically rich, with two key features – (i) the droplet and its self-generated wave coexist as a *wave-particle entity* (WPE); the droplet creates localized waves which in turn guide the droplet motion, and (ii) the system is non-Markovian and has *memory* since the waves generated by the droplet can decay very slowly in time and hence the droplet motion is affected by the history of waves along the droplet’s trajectory. Such WPEs exhibit hydrodynamic quantum analogs [19–22] and some examples include quantization of orbits [23–28], tunneling across submerged barriers [29–31], wave-like statistics in confined geometries [32–36], Friedel oscillations [37] and hydrodynamic superradiance [38, 39]. Most of the hydrodynamic quantum analogs have focused on a single WPE system, and investigations of many interacting WPEs have been limited [40–44]. In this Letter, we investigate strongly interacting clusters of WPEs and demonstrate that such active clusters exhibit hydrodynamic nuclear analogs.

Model—Consider N identical droplets (particles) bouncing periodically on a vertically vibrating bath of the same liquid while also moving horizontally in two dimensions $\mathbf{x} = (x, y)$. By averaging over the fast time scale of vertical periodic bouncing, Oza *et al.* [45] developed a theoretical stroboscopic model that provides a continuum description of the horizontal walking motion of a WPE as an integrodifferential equation. Let the i th particle be located at horizontal position \mathbf{x}_{pi} and move with horizontal velocity $\dot{\mathbf{x}}_{pi}$ while continuously generat-

ing axisymmetric standing waves that are centered at the particle location, have spatial structure $W(|\mathbf{x}|)$ and decay exponentially in time. This results in the dimensionless equation of motion [45]

$$\ddot{\mathbf{x}}_{pi} + \dot{\mathbf{x}}_{pi} = F_{ii}^{int} + \sum_{\substack{j=1 \\ j \neq i}}^N (F_{ij}^{int} + F_{ij}^{rep}) \quad (1)$$

for the horizontal dynamics of the i th WPE, where an overdot denotes a time derivative, and

$$F_{ij}^{int} = -R \int_{-\infty}^t W'(|\mathbf{x}_{pi}(t) - \mathbf{x}_{pj}(s)|) \frac{\mathbf{x}_{pi}(t) - \mathbf{x}_{pj}(s)}{|\mathbf{x}_{pi}(t) - \mathbf{x}_{pj}(s)|} e^{-\frac{(t-s)}{\tau}} ds,$$

$$F_{ij}^{rep} = K \frac{\mathbf{x}_{pi}(t) - \mathbf{x}_{pj}(t)}{|\mathbf{x}_{pi}(t) - \mathbf{x}_{pj}(t)|} (a - |\mathbf{x}_{pi}(t) - \mathbf{x}_{pj}(t)|),$$

when $|\mathbf{x}_{pi} - \mathbf{x}_{pj}| < a$ and $F_{ij}^{rep} = 0$ otherwise, with a as the particle diameter. The left-hand-side of Eq. (1) is composed of an inertial term and an effective drag force. The first term F_{ii}^{int} on the right-hand-side of the equation captures the forcing on the particle from its self-generated wave field. This force is proportional to the gradient of the self-generated wave field and it is calculated through integration of the individual wave forms $W(|\mathbf{x}|)$ that are continuously generated by the particle along its trajectory and decay exponentially in time. We choose this wave form to be $W(|\mathbf{x}|) =$

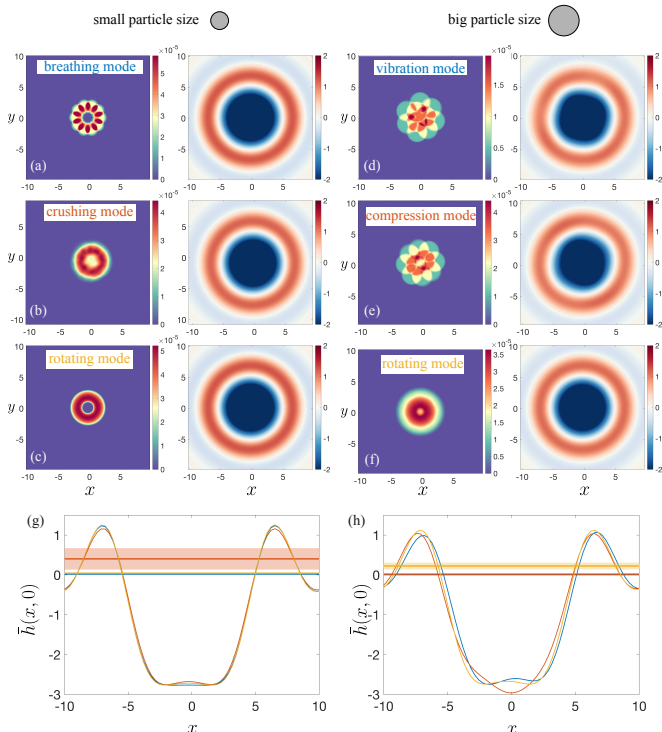


FIG. 3. Probability density of particles and the time-averaged wave field for different excitation modes. The time-averaged probability distribution of both (left) finite-size particle positions and (right) the underlying collective wave field corresponding to the excitation modes in Fig. 2 is shown in (a)-(f). (g) and (h) show the mean cluster kinetic energy \bar{E} (solid line) with their time-averaged collective potential for different modes for small particle size in (a)-(c) and large particle size in (d)-(f). Shaded regions indicate the uncertainty in the \bar{E} calculated as the standard deviation.

$\cos(|\mathbf{x}|) \exp[-(|\mathbf{x}|/2l)^2]$, with l as the length scale of spatial decay (see Fig. 1(a)). This wave form captures features of both spatial oscillations and spatial decay that are present in experiments [46]. The second term on the right hand side, F_{ij}^{int} , is the force on the i th particle due to the wave field of the j th particle. The last term on the right hand side is a repulsive spring force F_{ij}^{rep} that acts at short range and captures the finite size of the particle; we fix $K = 1000$. To non-dimensionalize the equation, spatial length is scaled by the inverse of the wavenumber $k_F = 2\pi/\lambda_F$ with λ_F as the wavelength of particle-generated waves, and time t is scaled by m/D where m is the particle mass and D is an effective drag coefficient. Dimensionless parameters R and τ denote the non-dimensional wave-amplitude and non-dimensional decay rate of waves, i.e. the memory time of the waves, respectively [47]. See Secs. I and II of the Supplemental Material [48] for details of non-dimensionalization and numerical implementation.

Active wave-particle clusters—For fixed R , an isolated WPE is stationary for small τ and undergoes a pitchfork bifurcation at a critical memory to a steady walking

state [45] (see Fig. 1(b)). Even when an isolated WPE is in a steady walking state, we find that a cluster of identical strongly interacting WPEs can spontaneously self-organize into a tightly bound cluster as shown in Fig. 1(c) and also observed in experiments with superwalking droplets (see Fig. 1(d) and Supplemental Video S9 of Ref. [13]). The collective wave field generated by the cluster of WPEs results in the emergence of a self-generated potential well near the core of the active cluster and a weak self-generated wave barrier surrounding the cluster. Moreover, the time-averaged wave field, with its self-generated wave barrier and associated self-generated potential well, exhibits features analogous to certain key aspects of the bag model for hadrons [49–51]. In both cases, we have a circular/spherical region within which the potential is approximately uniform and negative relative to the outside of the said region, with a confining potential barrier at the boundary between the interior and exterior of the bag. Parallels also exist with mean-field shell-model nuclear potentials, for the near-uniform negative potential in the cluster interior, and the repulsion-induced “bump” at the cluster edge [52].

We explore in detail an example of a cluster of ten WPEs as the memory parameter τ is varied for two different particle sizes: $a = 1.01$ (“small”) – a typical size of a walker [17, 53], and $a = 1.63$ (“big”) – a typical size of a superwalker [13]. At very small values for τ , the cluster of particles self-organizes into a static equilibrium structure (see Sec. III of [48]). As memory is progressively increased, different excitation modes emerge as shown in Fig. 2; such collective excitations vary with particle size. We quantify the shape dynamics of the cluster by fitting an ellipse to the centers of the particles and extracting the eccentricity e and inclination angle ϕ of the fitted ellipse as a function of time. For small particles of size $a = 1.01$, a static ring structure at very low memory transitions to a breathing mode as memory is increased (see Video S1) where WPEs oscillate radially as shown in Fig. 2(a). Here, the eccentricity e of the cluster is almost zero so the cluster remains circular but its average radius $\langle R \rangle$, calculated as the mean of the radial distance of each particle from the center of the cluster, oscillates with time (shown by yellow arrows between two dashed circles). We note that static ring configurations and radial oscillations have been observed in both experiments and simulations with rings of WPEs [42]. Further increase in memory gives a crushing mode where the fitted ellipse oscillates between two extremely deformed states whose inclination differs by almost $\pi/2$ rad (see Video S2 and Fig. 2(b)). At even higher memories, a rotating mode is observed where particles in the cluster self-organize into a deformed ring and the fitted ellipse rotates at almost a constant rate, i.e. $\dot{\phi}$ is constant and e is almost constant (see Video S3 Fig. 2(c)). Note, intermediate memory values correspond to a transition between these collective modes; one finds in general chaotic states of the active cluster along with a random-walk-like motion of its center of mass (see Sec. IV of the Supplemental Material [48] and Video S7).

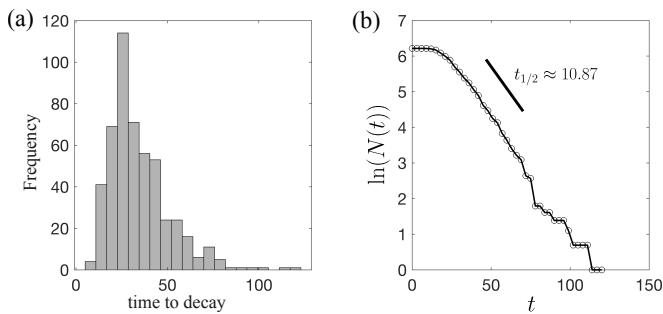


FIG. 4. Statistics of active wave-particle cluster decay. At large values of the memory parameter $\tau = 7.31$, clusters of bigger particles with $a = 1.63$ and $R = 1.72$ disintegrate by ejecting one or more particles. We show the distribution of (a) time of first particle decay and (b) number of undecayed clusters as a function of time. The number of undecayed clusters appears to follow an exponential decay law $N(t) = N_0 e^{-\lambda t}$ with $\lambda \approx 0.06375$ and half life $t_{1/2} = \ln(2)/\lambda \approx 10.87$. These statistics were calculated from $N_0 = 500$ simulations with different random initial perturbations in particle position.

For the cluster of big particles of size $a = 1.63$, one first encounters a vibrating mode after the instability of the stationary cluster, as shown in Fig. 2(d) (see also Video S4). In this mode, particles in the cluster core oscillate with very small amplitudes whereas the ones near the boundary oscillate mainly in the angular direction θ with $\omega = \dot{\theta}$. Further increasing memory leads to a compression mode where, again, particles in the core stay static while the periphery particles oscillate radially inwards and outwards (see Video S5 and Fig. 2(e)). Hence, the entire cluster oscillates between circular and elliptical shapes. At higher memory, we also see the rotating mode for the bigger particles (see Video S6 and Fig. 2(f)). For memory values just before the onset of a steady rotation mode, an intermittent rotation mode is observed where the cluster intermittently switches between clockwise and counterclockwise rotation (see Sec. IV of the Supplemental Material [48] and Video S8). Thus, we obtain excitation modes of the collective cluster, which are reminiscent of various excitation modes in different quantum-mechanical models for nuclei, such as the shell or liquid droplet models [54].

We now turn to the statistics of WPEs for these excitation modes. Figure 3(a)-(f) shows the probability density of particles (left)[55] and time-averaged collective wave field (right) for each excitation mode of both particle sizes in Fig. 2. We find that although the probability density for particles is different in each mode due to the different dynamics, the time-averaged wave field, and hence the average potential of the collective cluster, is approximately the same for all excitation modes (see also Sec. V of Supplemental Material [48]).

Such behavior is analogous to the hadron bag model [49–51]. We also calculate the kinetic energy of the cluster $E(t) = (1/N) \sum_{i=1}^N |\dot{\mathbf{x}}_{pi}|^2$ and time-average over the duration of the simulation to obtain the mean cluster kinetic energy \bar{E} . Plotting \bar{E} in the time-averaged potential well form (see Fig. 3(d) and (e)), we obtain energy level diagrams analogous to different energy levels of nuclear excitation modes [54]. We find that some of these different dynamical modes have almost similar mean kinetic energies making the energy levels degenerate, while other modes have different mean kinetic energies.

Active cluster decay—For larger values of memory beyond the rotating mode, one finds that clusters of small particle size $a = 1.01$ dynamically stabilize into a static ring configuration. Conversely, at high memory the bigger particle cluster ($a = 1.63$) undergoes vigorous fluctuations and spontaneously starts ejecting particles (as observed for superwalkers; see Supplemental Video S9 of [13] and Videos in [56]), analogous to radioactive nuclear decay. After ejection, the particle can either stay weakly bound outside the cluster or completely escape the cluster (see Sec. VI of the Supplemental Material [48] and Videos S9-S10). The weakly bound particle orbiting the cluster is analogous to halo nuclei [57] where a core atomic nucleus is surrounded by a halo of orbiting hadrons. To quantify particle decay statistics, we plot the distribution of ejection time for first particle from the cluster, as well as the number of non-decayed clusters with time, in Fig. 4. We find that the distribution of the time taken for first particle decay has a Poisson-like distribution. The time series of the number of non-decayed clusters with time follows an exponential decay, similar to radioactive nuclear decay, with half-life $t_{1/2} \approx 10.87$.

Conclusions—We showed that multiple WPEs can self-organize into nucleus-like structures which exhibit various modes of collective excitation as the system memory increases. These various excitations give rise to a similar time-averaged collective wave field which allows us to draw connections with nuclear bag models. Further, at large memory, WPE clusters can spontaneously emit particles which follows exponential decay laws similar to radioactive decay. Our work opens avenues to explore in detail hydrodynamic nuclear analogs in both experiments and simulations with WPEs (see Sec. VII of Supplemental Material [48] for a discussion). For example, it would be interesting to investigate analogs of stable and unstable nuclei by investigating the stability of differently sized WPE clusters, and analogs of nuclear scattering.

Acknowledgments—R.V. acknowledges the support of the Leverhulme Trust [Grant No. LIP-2020-014] and the ERC Advanced Grant ActBio (funded as UKRI Frontier Research Grant EP/Y033981/1).

[1] V. I. Strazhev and P. L. Shkol'nikov, Electrodynamics without potentials, Sov. Phys. J. **32**, 378 (1989).

[2] B. S. DeWitt, Quantum theory without electromagnetic

- potentials, *Phys. Rev.* **125**, 2189 (1962).
- [3] R. M. Wald, *Advanced Classical Electromagnetism* (Princeton University Press, Princeton, 2022) pp. 8–9.
- [4] J. D. Jackson, *Classical Electrodynamics*, 3rd ed. (John Wiley & Sons, Hoboken, 1999).
- [5] P. A. M. Dirac, Classical theory of radiating electrons, *Proc. R. Soc. Lond. A* **167**, 148 (1938).
- [6] E. Merzbacher, *Quantum Mechanics*, 3rd ed. (Wiley, New York, 1998) pp. 560–564.
- [7] M. Fabre de La Ripelle and H. Fiedeldey, An integro-differential equation approach to the many-body problem, *Phys. Lett. B* **171**, 325 (1986).
- [8] M. Fabre de la Ripelle, H. Fiedeldey, and S. A. Sofianos, Integrodifferential equation for few- and many-body systems, *Phys. Rev. C* **38**, 449 (1988).
- [9] W. Oehm, S. A. Sofianos, H. Fiedeldey, and M. Fabre de la Ripelle, Integrodifferential equation approach. I. Triton and α -particle binding energies, *Phys. Rev. C* **42**, 2322 (1990).
- [10] W. Oehm, S. A. Sofianos, H. Fiedeldey, and M. Fabre de la Ripelle, Integro-differential equation approach. II. Triton and α -particle wave functions, graphical plots, *Phys. Rev. C* **43**, 25 (1991).
- [11] W. Oehm, H. Fiedeldey, S. A. Sofianos, and M. Fabre de la Ripelle, Integro-differential equation approach. III. Triton and α -particle bound states. realistic forces and two-body correlations, *Phys. Rev. C* **44**, 81 (1991).
- [12] R. M. Adam, S. A. Sofianos, H. Fiedeldey, and M. F. de la Ripelle, Integro-differential equation approach extended to larger nuclei, *J. Phys. G: Nucl. Part. Phys.* **18**, 1365 (1992).
- [13] R. N. Valani, A. C. Slim, and T. Simula, Superwalking droplets, *Phys. Rev. Lett.* **123**, 024503 (2019).
- [14] S. Ramaswamy, The mechanics and statistics of active matter, *Annu. Rev. Condens. Matter Phys.* **1**, 323 (2010).
- [15] L. Pismen, Active colloids, in *Active Matter Within and Around Us: From Self-Propelled Particles to Flocks and Living Forms* (Springer International Publishing, Cham, 2021) pp. 43–64.
- [16] L. Pismen, Motion of microorganisms, in *Active Matter Within and Around Us: From Self-Propelled Particles to Flocks and Living Forms* (Springer International Publishing, Cham, 2021) pp. 65–90.
- [17] Y. Couder, S. Protière, E. Fort, and A. Boudaoud, Dynamical phenomena: Walking and orbiting droplets, *Nature* **437**, 208 (2005).
- [18] S. Protière, A. Boudaoud, and Y. Couder, Particle-wave association on a fluid interface, *J. Fluid Mech.* **554**, 85–108 (2006).
- [19] J. W. M. Bush, Pilot-wave hydrodynamics, *Annu. Rev. Fluid Mech.* **47**, 269 (2015).
- [20] J. W. M. Bush and A. U. Oza, Hydrodynamic quantum analogs, *Rep. Prog. Phys.* **84**, 017001 (2020).
- [21] J. W. M. Bush, K. Papatryfonos, and V. Frumkin, The state of play in hydrodynamic quantum analogs, in *Advances in Pilot Wave Theory: From Experiments to Foundations*, edited by P. Castro, J. W. M. Bush, and J. Croca (Springer International Publishing, Cham, 2024) pp. 7–34.
- [22] J. W. M. Bush, V. Frumkin, and P. J. Sáenz, Perspectives on pilot-wave hydrodynamics, *Appl. Phys. Lett.* **125**, 030503 (2024).
- [23] E. Fort, A. Eddi, A. Boudaoud, J. Moukhtar, and Y. Couder, Path-memory induced quantization of classical orbits, *Proc. Natl. Acad. Sci.* **107**, 17515 (2010).
- [24] D. M. Harris and J. W. M. Bush, Droplets walking in a rotating frame: from quantized orbits to multimodal statistics, *J. Fluid Mech.* **739**, 444–464 (2014).
- [25] A. U. Oza, D. M. Harris, R. R. Rosales, and J. W. M. Bush, Pilot-wave dynamics in a rotating frame: on the emergence of orbital quantization, *J. Fluid Mech.* **744**, 404 (2014).
- [26] S. Perrard, M. Labousse, E. Fort, and Y. Couder, Chaos driven by interfering memory, *Phys. Rev. Lett.* **113**, 104101 (2014).
- [27] S. Perrard, M. Labousse, M. Misikin, E. Fort, and Y. Couder, Self-organization into quantized eigenstates of a classical wave-driven particle, *Nat. Commun.* **5**, 3219 (2014).
- [28] M. Labousse, S. Perrard, Y. Couder, and E. Fort, Self-attraction into spinning eigenstates of a mobile wave source by its emission back-reaction, *Phys. Rev. E* **94**, 042224 (2016).
- [29] A. Eddi, E. Fort, F. Moisy, and Y. Couder, Unpredictable tunneling of a classical wave-particle association, *Phys. Rev. Lett.* **102**, 240401 (2009).
- [30] A. Nachbin, P. A. Milewski, and J. W. M. Bush, Tunneling with a hydrodynamic pilot-wave model, *Phys. Rev. Fluids* **2**, 034801 (2017).
- [31] L. Tadrast, T. Gilet, P. Schlagheck, and J. W. M. Bush, Predictability in a hydrodynamic pilot-wave system: Resolution of walker tunneling, *Phys. Rev. E* **102**, 013104 (2020).
- [32] D. M. Harris, J. Moukhtar, E. Fort, Y. Couder, and J. W. M. Bush, Wavelike statistics from pilot-wave dynamics in a circular corral, *Phys. Rev. E* **88**, 011001 (2013).
- [33] T. Gilet, Quantumlike statistics of deterministic wave-particle interactions in a circular cavity, *Phys. Rev. E* **93**, 042202 (2016).
- [34] P. J. Sáenz, T. Cristea-Platon, and J. W. M. Bush, Statistical projection effects in a hydrodynamic pilot-wave system, *Nat. Phys.* **14**, 315 (2018).
- [35] T. Cristea-Platon, P. J. Sáenz, and J. W. M. Bush, Walking droplets in a circular corral: Quantisation and chaos, *Chaos* **28**, 096116 (2018).
- [36] M. Durey, P. A. Milewski, and Z. Wang, Faraday pilot-wave dynamics in a circular corral, *J. Fluid Mech.* **891**, A3 (2020).
- [37] P. J. Sáenz, T. Cristea-Platon, and J. W. M. Bush, A hydrodynamic analog of Friedel oscillations, *Sci. Adv.* **6** (2020).
- [38] K. Papatryfonos, M. Ruelle, C. Bourdiol, A. Nachbin, J. W. M. Bush, and M. Labousse, Hydrodynamic super-radiance in wave-mediated cooperative tunneling, *Commun. Phys.* **5**, 142 (2022).
- [39] V. Frumkin, J. W. M. Bush, and K. Papatryfonos, Superradiant droplet emission from parametrically excited cavities, *Phys. Rev. Lett.* **130**, 064002 (2023).
- [40] A. Hélias and M. Labousse, Statistical self-organization of an assembly of interacting walking drops in a confining potential, *The European Physical Journal E* **46**, 29 (2023).
- [41] T. P. Simula, Droplet time crystals, *Phys. Scr.* (2023).
- [42] M. M. P. Couchman and J. W. M. Bush, Free rings of bouncing droplets: stability and dynamics, *Journal of Fluid Mechanics* **903**, A49 (2020).
- [43] S. Protière, Y. Couder, E. Fort, and A. Boudaoud, The

- self-organization of capillary wave sources, *Journal of Physics: Condensed Matter* **17**, S3529 (2005).
- [44] A. Eddi, A. Boudaoud, and Y. Couder, Oscillating instability in bouncing droplet crystals, *Europhysics Letters* **94**, 20004 (2011).
- [45] A. U. Oza, R. R. Rosales, and J. W. M. Bush, A trajectory equation for walking droplets: hydrodynamic pilot-wave theory, *J. Fluid Mech.* **737**, 552 (2013).
- [46] A. P. Damiano, P.-T. Brun, D. M. Harris, C. A. Galeano-Rios, and J. W. M. Bush, Surface topography measurements of the bouncing droplet experiment, *Experiments in Fluids* **57**, 163 (2016).
- [47] R. N. Valani, Infinite-memory classical wave-particle entities, attractor-driven active particles, and the diffusionless Lorenz equations, *Chaos* **34**, 013133 (2024).
- [48] See Supplemental Material at [URL will be inserted by publisher] for non-dimensionalization of equation of motion (Sec. I), details of numerical implementation (Sec. II), cluster configurations at low-memory (Sec. III), results in chaotic excitations (Sec. IV), convolution results for time-averaged wavefield (Sec. V), cluster decay dynamics (Sec. VI) and comments on further connections with nuclear physics (Sec. VII).
- [49] P. N. Bogolioubov, Sur un modèle à quarks quasi-indépendants, *Annales de l'institut Henri Poincaré. Section A, Physique Théorique* **8**, 163 (1968).
- [50] A. Chodos, R. L. Jaffe, K. Johnson, C. B. Thorn, and V. F. Weisskopf, New extended model of hadrons, *Phys. Rev. D* **9**, 3471 (1974).
- [51] A. Chodos, R. L. Jaffe, K. Johnson, and C. B. Thorn, Baryon structure in the bag theory, *Phys. Rev. D* **10**, 2599 (1974).
- [52] B. L. Cohen, *Concepts of Nuclear Physics* (McGraw-Hill, 1971) p. 67.
- [53] J. Moláček and J. W. M. Bush, Drops walking on a vibrating bath: towards a hydrodynamic pilot-wave theory, *J. Fluid Mech.* **727**, 612 (2013).
- [54] K. S. Krane, *Introductory Nuclear Physics* (Wiley, 1987).
- [55] The finite size of the particle as a disc of diameter a is taken into account while calculating the probability density.
- [56] R. Valani, A. C. Slim, and T. Simula, Superwalkers, Monash University. Media <https://doi.org/10.26180/5d393111595db> (2020).
- [57] Y. Ye, X. Yang, H. Sakurai, and B. Hu, Physics of exotic nuclei, *Nat. Rev. Phys.* **7**, 21 (2025).